Int. J. Adv. Appl. Math. and Mech. 6(2) (2018) 30 – 41 (ISSN: 2347-2529)

Journal homepage: www.ijaamm.com

IJAAMM

International Journal of Advances in Applied Mathematics and Mechanics

Cell and patch vicinity travel restrictions in a multi-regions SI discrete epidemic control model

Research Article

Omar Zakary, Sara Bidah, Mostafa Rachik, Ilias Elmouki*

Department of Mathematics and Computer Science, Hassan II University of Casablanca. BP 7955, Sidi Otheoreman, Casablanca, Morocco

Received 21 September 2018; accepted (in revised version) 27 November 2018

Abstract: Some epidemics can spread in geographical large scales and in unprecedented durations if the authorities concerned do not hurry to save susceptible populations. In such cases, mathematical modelers are required to take into account the spatial aspect of the propagation of an epidemic. Infected travelers either exiting the main source of epidemic or coming from other locations that have been partially affected later, and aiming to enter safer regions, represent the population category that should be hastily controlled. Based on these assumptions, and with the consideration of the factor of their mobility, we devise a discrete-time Susceptible-Infected (SI) model which describes the spatial spread of an epidemic emerging in regions that are connected by any kind of movement. Furthermore, we introduce into SI discrete equations, controls variables which restrict movements of infected people for avoiding any contact with the susceptible class. Explicitly, we present regions by M^2 cells assembled in one grid, and we seek the optimal values of controls using a discrete version of Pontryagin's maximum principle. In a first case, we aim to control only one cell by restricting movements of infected people coming from its neighbors, and in a second case, we aim to control a group of cells or patches, based on the same logic of inter-interventions and which is related to the vicinity travel restrictions optimal control strategy. In a first time, the patch is supposed to be located in the opposite side of the epidemic source, and in a second time, in the interior of the domain of study in order to verify the effectiveness of such control policies when the number of regions in the vicinity set, is either small or important.

MSC: 93C15 • 34B15

Keywords: Spatial spread of epidemic • Discrete-time model • SI epidemic model • Multi-regions • Optimal control • travel restrictions • Vicinity • Cell • Patch

1. Introduction

Devised in 1927 by Kermack and McKendrick [1], Susceptible-Infected-Removed (SIR) systems still interest many researchers in mathematical epidemiology [2],[3],[4],[5],[6]. On the other hand, there are SI epidemic models which do not assume the presence of a removed class of population and where there is no hypothesis that after a short time of healing from the disease, an infected individual could move again to the susceptible compartment as in SIS systems [7],[8],[9]. In fact, SI models, represent the simplest compartmental systems in this area of research. Nowadays, this type of models is adapted and applied to many different subjects, see for examples, studies treated in [10],[11],[12].

Recent epidemic models based on multi-regions discrete-time SIR models, have been devised in [13],[14] with extending their modeling approach in the continuous-time case with applications in HIV/AIDS and Ebola epidemics as in [15],[16], all for the study of the spatial-temporal spread of epidemics which emerge in different geographical

* Corresponding author.
E-mail address(es): i.elmouki@gmail.com (Ilias Elmouki).

regions and also, in attempt to exhibit the influence of one region on an other region via infection movement. The authors have also applied their modeling concept to cases of SIR, SIS, SIRS and SEIRS systems as in [17],[18],[19],[20]. Models in these last four references and in [13],[14], were all in the form of discrete-time systems. In fact, as noted in [13] and [21], the consideration of difference equations rather than differential equations, is due to the fact that epidemiological data are often collected at discrete times.

In this paper, we take into account the spatial spread of an epidemic within the studied domain denoted Ω, and which is divided into different regions or cells, uniform in size and denoted $C_{pq}, p, q = 1, ..., M$ (see Fig. 1(a)), and which are supposed to be connected by movements, and could illustrate even the case of detached regions even if they are observed assembled in one grid. For each cell C_{pq} a discrete SI model is formulated, in order to characterize the state of the epidemic in different places of Ω.

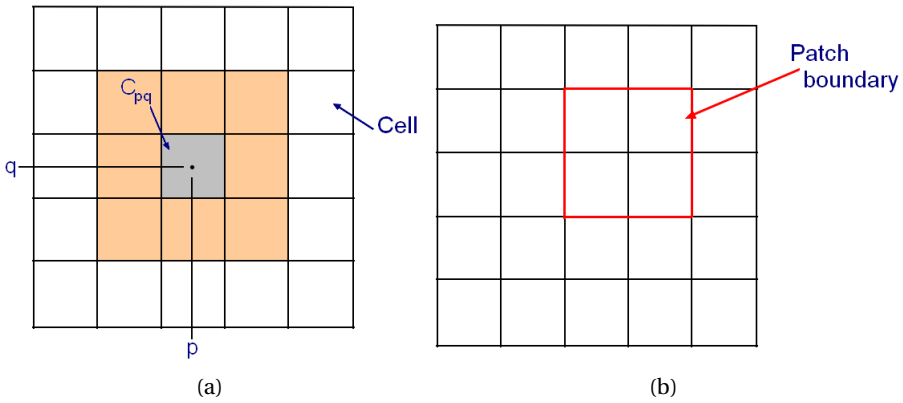

Fig. 1. Cells grid of Ω. (a) The colored contour of C_{pq} represents its vicinity set denoted by V_{pq}. (b) An example of a group of 4 cells or patch.

The main goal of this work is formulate an optimal control problem relative to multi-regions discrete-time SI models in cells and patches, without specifying the name of the epidemic. Thus, a novel control application is provided for the analysis of spatial control strategies for all epidemics that could spread rapidly in many places. For this, it is assumed here, that the epidemic can be transmitted and propagated from one spatial cell C_{pq} to its vicinity V_{pq} (see Fig. 1(a)) by movements of people. We consider a control objective which aims to reduce the spread of the epidemic within Ω, by introducing blocker controls variables in the discrete-time SI model corresponding to the cell aiming to control. These controls restrict movements of infected individuals coming from the vicinity set associated to the targeted cell, in order to limit contacts between its susceptible people with the infected ones. As a second task, we try to control several cells that belong to small geographical locations (patches: see Fig. 1(b)). The optimal control strategy is named the travel-blocking vicinity optimal control approach, as in [17], [18], [19], [20].

In order to illustrate the effectiveness of the proposed modeling and control approaches when they are applied to cells, we give examples associated to two cases of the source of infection: 1. when the epidemic starts from one corner of the grid (i.e. a cell with 3 neighbors), and 2. when it starts far away of the corner or near the center of the considered domain (i.e. a cell with 8 neighbors), while the cell which is targeted by our control strategy, has 8 neighbors. As regards to simulations of patches as previously studied in the case of SIR model [22], we investigate here the two same mentioned cases 1. and 2. in our SI model but with the consideration of a patch which contains 4 joined cella, once with 5 neighbors in the intersection between the vicinity of its cells and its complementary set, and an other time, with 12 neighbors.

The rest of the manuscript is organized as follows: In Section 2., we describe the mathematical model. The objective functional and the analysis of optimal control approach associated to the case when only one cell is controlled, are given in Section 3. with the introduction of numerical simulations. Section 4. includes the analysis of the optimal control problem in case of a patch. Finally, we conclude our work in Section 5.

2. Mathematical SI multi-regions model

Consider a discrete-time SI model model within a domain Ω, occupied by an homogeneous population and divided to M^2 cells, uniform in size (see Fig. 1), i.e. $\Omega = \bigcup_{p,q=1,..,M} C_{pq}$, where C_{pq} denoting a spatial location. According to the disease transmission mechanism, the host population of each cell C_{pq} is grouped into two epidemiological compartments, $S_i^{C_{pq}}$; susceptible individuals, and $I_i^{C_{pq}}$; infected individuals, at instant i. We assume that the suscep-

tible individuals of C_{pq} are not yet infected but can be infected only through contacts with infectives of C_{pq} and V_{pq} (Neighborhood or Vicinity of C_{pq}, see Fig. 1), thus, the infection transmission is assumed to occur between individuals that are present in a given cell C_{pq}. Its rate is given by

$$\sum_{C_{rs} \in V_{pq}} \beta_{rs} I_i^{C_{rs}} S_i^{C_{pq}}$$

where β_{rs} is a constant proportion of contacts between a susceptible from a cell C_{pq} and an infective from its neighbor cell $C_{rs} \in V_{pq}$ with $V_{pq} = \{C_{rs} \in \Omega / r = p + k, s = p + k', k, k' \in \{-1, 0, 1\}\}$, a Moor neighborhood type.

The following system describes the multi-cells discrete SI model corresponding to cell C_{pq}

$$S_{i+1}^{C_{pq}} = S_i^{C_{pq}} - \sum_{C_{rs} \in V_{pq}} \beta_{rs} I_i^{C_{rs}} S_i^{C_{pq}} - d S_i^{C_{pq}} \tag{1}$$

$$I_{i+1}^{C_{pq}} = I_i^{C_{pq}} + \sum_{C_{rs} \in V_{pq}} \beta_{rs} I_i^{C_{rs}} S_i^{C_{pq}} - (d + \alpha + \gamma) I_i^{C_{pq}} \tag{2}$$

$$S_0^{C_{pq}} \geq 0, \quad I_0^{C_{pq}} \geq 0 \quad are\ given \tag{3}$$

For $p, q = 1, 2, ..., M$, $d > 0$ is the natural death rate, $\alpha > 0$ is the death rate due to the infection, $\gamma > 0$ denotes the recovery rate of infectives. By assuming that Ω is occupied by an homogeneous population, d, α and γ are assumed to be the same for all cells of Ω.

3. Methods I: Control of one cell

3.1. Presentation of the model with controls

We introduce control variables $u_i^{C_{rs}}$ $(C_{rs} \in V_{pq})$ in the above mentioned model (1-3), in order to limit access to the controlled cell. In other words, control variables are introduced for restricting contacts between susceptible people of the targeted cell C_{pq} and infected individuals of the other cells from V_{pq}. Then, for a given cell C_{pq} in Ω, the model is given by the following equations

$$S_{i+1}^{C_{pq}} = S_i^{C_{pq}} - \beta_{pq} I_i^{C_{pq}} S_i^{C_{pq}} - \sum_{C_{rs} \in V_{pq}} u_i^{C_{rs}} \beta_{rs} I_i^{C_{rs}} S_i^{C_{pq}} - d S_i^{C_{pq}} \tag{4}$$

$$I_{i+1}^{C_{pq}} = I_i^{C_{pq}} + \beta_{pq} I_i^{C_{pq}} S_i^{C_{pq}} + \sum_{C_{rs} \in V_{pq}} u_i^{C_{rs}} \beta_{rs} I_i^{C_{rs}} S_i^{C_{pq}} - (d + \alpha + \gamma) I_i^{C_{pq}} \tag{5}$$

$$S_0^{C_{pq}} \geq 0, \qquad I_0^{C_{pq}} \geq 0 \qquad are\ given \tag{6}$$

Control functions are assumed taking values between u^{min} and u^{max} , where $u^{max} < 1$ and $u^{min} > 0$.

3.2. A vicinity travel restrictions optimal control approach on cells

The problem concerns the minimization of the following objective functional

$$J_{pq}(u) = A I_N^{C_{pq}} + \sum_{i=0}^{N-1} \left(A I_i^{C_{pq}} + \sum_{C_{rs} \in V_{pq}} \frac{A_{rs}}{2} (u_i^{C_{rs}})^2 \right) \tag{7}$$

Where $u = \left(u_i^{C_{rs}}\right)_{C_{rs} \in V_{pq},\, i=0,...,N-1}$. In fact, we aim to minimize the infectives, while minimizing the cost of the vicinity travel restrictions control strategy in the cell C_{pq}. The quadratic cost is chosen for simplicity and other forms could be treated similarly. The minimization control problem is taken over controls set,

$$U = \left\{ u \text{ measurable} / u^{min} \leq u_i^{C_{rs}} \leq u^{max},\ i = 1, ..., N-1,\ C_{rs} \in V_{pq} \right\}$$

Thus, we seek an optimal control $u^* = \left(u_i^{C_{rs}*}\right)_{C_{rs} \in V_{pq},\, i=1,...,N-1} \in U$ which minimizes the objective functional (7).

An optimal control exists due to the finite dimensional structure of this system. The sufficient conditions of optimality in an example of a discrete-time epidemic model, have been stated and proven in [21]. Since similar analysis process can be followed for our example here, we omit the proof of this part here. The necessary conditions that an optimal control and corresponding states must satisfy are characterized by using discrete version of the Pontryagin's maximum principle [23]. The adjoint variables are used to attach the difference equations to the considered minimization problem. As in optimal control of ordinary differential equations, we can obtain the necessary conditions from the Hamiltonian H. In the discrete version, at each time $i < N$, the Hamiltonian is formed from the terms in the objective functional (at time i), and the adjoint variables (at time $i+1$) multiplying the corresponding right-hand side of the difference equations. Thus, for a cell C_{pq}, the Hamiltonian is given by

$$\begin{aligned} H &= AI_i^{C_{pq}} + \sum_{C_{rs}\in V_{pq}} \frac{A_{rs}}{2}(u_i^{C_{rs}})^2 \\ &+ \zeta_{1,i+1}^{C_{pq}}\left[S_i^{C_{pq}} - \beta_{pq} I_i^{C_{pq}} S_i^{C_{pq}} - \sum_{C_{rs}\in V_{pq}} u_i^{C_{rs}}\beta_{rs} I_i^{C_{rs}} S_i^{C_{pq}} - dS_i^{C_{pq}}\right] \\ &+ \zeta_{2,i+1}^{C_{pq}}\left[I_i^{C_{pq}} + \beta_{pq} I_i^{C_{pq}} S_i^{C_{pq}} + \sum_{C_{rs}\in V_{pq}} u_i^{C_{rs}}\beta_{rs} I_i^{C_{rs}} S_i^{C_{pq}} - (d+\alpha+\gamma) I_i^{C_{pq}}\right] \end{aligned}$$

In the following, we announce the theorem of characterization of the optimal control u^* along with the necessary conditions

Theorem 3.1.
(Necessary Conditions) Given an optimal control u^* and solutions $S^{C_{pq}*}$ and $I^{C_{pq}*}$, there exists $\zeta_{k,i}^{C_{pq}}$, $i = 0...N$, $k = 1,2$, the adjoint variables satisfying the following equations

$$\triangle\zeta_{1,i}^{C_{pq}} = -\left[(1-d)\zeta_{1,i+1}^{C_{pq}} + \left(\beta_{pq} I_i^{C_{pq}} + \sum_{C_{rs}\in V_{pq}} u_i^{C_{rs}}\beta_{rs} I_i^{C_{rs}}\right)\left(\zeta_{2,i+1}^{C_{pq}} - \zeta_{1,i+1}^{C_{pq}}\right)\right] \tag{8}$$

$$\triangle\zeta_{2,i}^{C_{pq}} = -\left[A + \beta_{pq} S_i^{C_{pq}}\left(\zeta_{2,i+1}^{C_{pq}} - \zeta_{1,i+1}^{C_{pq}}\right) + (1-d-\alpha-\gamma)\zeta_{2,i+1}^{C_{pq}}\right] \tag{9}$$

where $\zeta_{1,N}^{C_{pq}} = 0$, $\zeta_{2,N}^{C_{pq}} = A$, are the transversality conditions. In addition

$$u_i^{C_{rs}*} = min\{max\{0, \frac{\left(\zeta_{1,i+1}^{C_{pq}} - \zeta_{2,i+1}^{C_{pq}}\right)\beta_{rs} I_i^{C_{rs}} S_i^{C_{pq}}}{A_{rs}}\}, u^{max}\},\ i = 0,...,N-1,\ C_{rs}\in V_{pq} \tag{10}$$

Proof. Based on results in [23], and setting $S^{C_{pq}} = S^{C_{pq}*}$, $I^{C_{pq}} = I^{C_{pq}*}$ and $u_i^{C_{rs}} = u_i^{C_{rs}*}$ we obtain the following adjoint equations

$$\begin{aligned} \triangle\zeta_{1,i}^{C_{pq}} &= -\frac{\partial\mathscr{H}}{\partial S_i^{C_{pq}}} = -\left[(1-d)\zeta_{1,i+1}^{C_{pq}} + \left(\beta_{pq} I_i^{C_{pq}} + \sum_{C_{rs}\in V_{pq}} u_i^{C_{rs}}\beta_{rs} I_i^{C_{rs}}\right)\left(\zeta_{2,i+1}^{C_{pq}} - \zeta_{1,i+1}^{C_{pq}}\right)\right] \\ \triangle\zeta_{2,i}^{C_{pq}} &= -\frac{\partial\mathscr{H}}{\partial I_i^{C_{pq}}} = -\left[A + \beta_{pq} S_i^{C_{pq}}\left(\zeta_{2,i+1}^{C_{pq}} - \zeta_{1,i+1}^{C_{pq}}\right) + (1-d-\alpha-\gamma)\zeta_{2,i+1}^{C_{pq}}\right] \end{aligned}$$

with $\zeta_{1,N}^{C_{pq}} = 0$, $\zeta_{2,N}^{C_{pq}} = A$. In order to characterize the optimal control u^*, we need to differentiate the Hamiltonian with respect to the control at each cell C_{rs} at time i and set it equal to zero, i.e.

$$\frac{\partial H}{\partial u_i^{C_{rs}}} = A_{rs} u_i^{C_{rs}} - \zeta_{1,i+1}^{C_{pq}}\beta_{rs} I_i^{C_{rs}} S_i^{C_{pq}} + \zeta_{2,i+1}^{C_{pq}}\beta_{rs} I_i^{C_{rs}} S_i^{C_{pq}} = 0$$

Then we obtain the optimal control

$$u_i^{C_{rs}} = \frac{\left(\zeta_{1,i+1}^{C_{pq}} - \zeta_{2,i+1}^{C_{pq}}\right)\beta_{rs} I_i^{C_{rs}} S_i^{C_{pq}}}{A_{rs}}$$

By the bounds in U of the control, it is easy to obtain $u_i^{C_{rs}*}$ in the following form

$$u_i^{C_{rs}*} = min\{max\{0, \frac{\left(\zeta_{1,i+1}^{C_{pq}} - \zeta_{2,i+1}^{C_{pq}}\right)\beta_{rs} I_i^{C_{rs}} S_i^{C_{pq}}}{A_{rs}}\}, u^{max}\},\ i = 0,...,N-1,\ C_{rs}\in V_{pq}$$

□

Table 1. Parameters values of α, β, γ and d, associated to a noninfected cell C_{pq}, $p,q = 1,...,M$, and which are utilized for the simulations obtained in all Figures below, with the initial conditions $S_0^{C_{pq}}$ and $I_0^{C_{pq}}$.

	S_0	I_0	α	β	γ	d
C_{pq}	40	0	0.002	0.0001	0.003	0.0001

3.3. Results I

We now present numerical simulations associated to the above mentioned optimal control problem. We write a code in MATLAB^M and simulate our results using data cited in Table 1. The optimality systems are solved using an iterative method. The state system with an initial guess is solved forward in time and then the adjoint system is solved backward in time because of the transversality conditions. Afterwards, the optimal controls values are updated using the values of state and costate variables obtained in the previous steps. Finally, we execute the previous steps till a tolerance criterion is reached.

In order to show the importance of our work, and without loss of generality, we consider a 9×9 grid. Initially ($i = 1$), susceptible people are homogeneously distributed with 40 in each cell except at the lower left corner cell C_{91}, where we introduce 5 infectives, and 35 susceptibles. Then, we investigate the case when the disease starts from the lower left corner of Ω, and at the cell C_{55} when the disease starts from the middle of Ω. In all figures below, the yellower the color-bars are the larger ones.

3.3.1. Without controls

Fig. 2(a) and Fig. 2(a), depict the behavior of the number of susceptible people without control when the disease starts from C_{91} and when it starts from C_{55}. It is observed in the first case, that at time $i = 600$, the epidemic has reduced the number of susceptible individuals, and then, susceptibles will disappear, while in the second case, the situation is more severe, which is reasonable, because the disease arrived at the upper right corner faster than the first case.

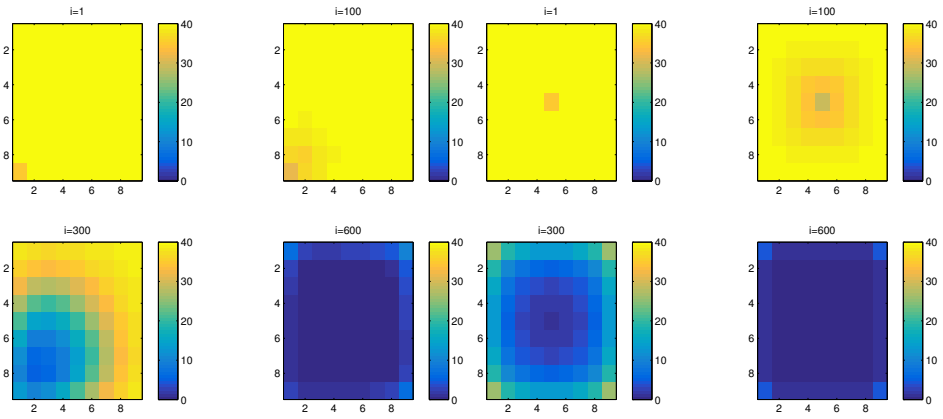

Fig. 2. Susceptibles behavior within Ω when there are no controls. (a) When the infection starts from the lower-left corner cell C_{91}. (b) When the infection starts from the middle cell C_{55}.

Fig. 3(a) and Fig. 3(b) in both cases, and we can observe that the number of infected individuals is rapidly increasing in the second case, while in both parts of the figure, there is a remarkable increase of infected individuals at time $i = 300$, followed by a decrease at time $i = 600$.

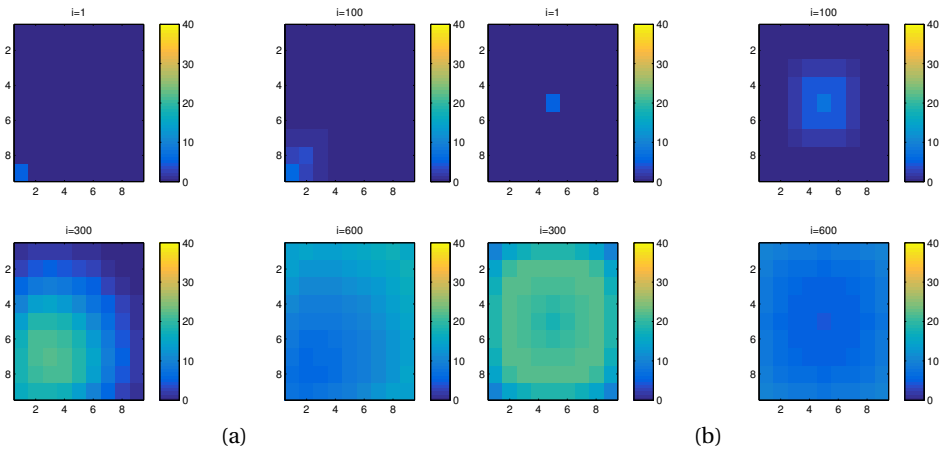

Fig. 3. Infectives behavior within Ω when there are no controls. (a) When the infection starts from the lower-left corner cell C_{91}. (b) When the infection starts from the middle cell C_{55}.

3.3.2. With controls

Now, we present numerical results associated to system (4)-(6) with the optimal control (10). We note that the target cell aiming to control here, is C_{83}. Fig. 4(a) and Fig. 4(b) show the behavior of the number of susceptible individuals with controls, and it is observed that the targeted cell C_{83} remains relatively insensitive to the spread of the epidemic, in the both cases (regardless of the infection source).

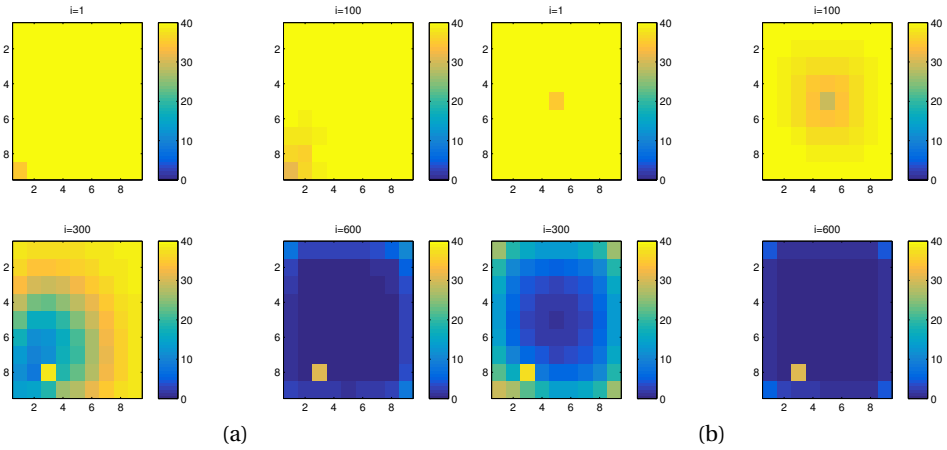

Fig. 4. Susceptibles behavior within Ω with controls. (a) When the infection starts from the lower-left corner cell C_{91}. (b) When the infection starts from the middle cell C_{55}.

Fig. 5(a) and Fig. 5(b) show the influence of the infected individuals of the controlled cell in the case where controls are used, and in this case, we can deduce that the number of infected individuals in C_{83} is sufficiently smaller than when there was yet no control strategy as in Fig. 3.

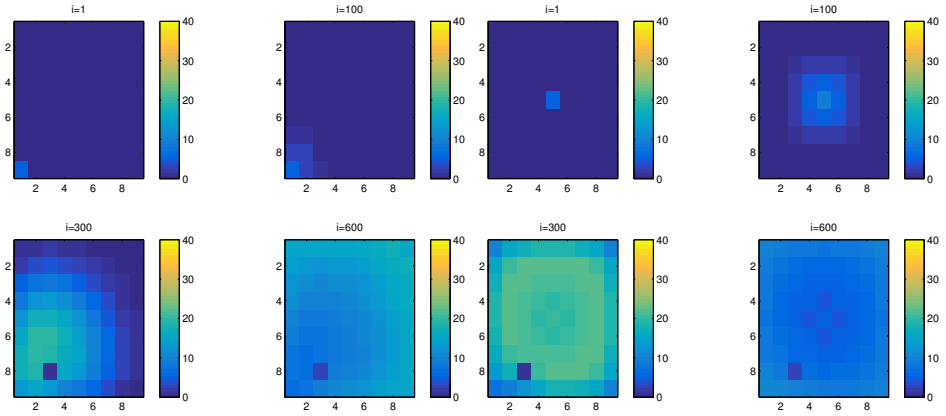

Fig. 5. Infectives behavior within Ω with controls. (a) When the infection starts from the lower-left corner cell C_{91}. (b) When the infection starts from the middle cell C_{55}.

4. Methods II: Control of patches

Let $I = \{1,2,...,M\}$ and $I_H \subset I$, set $P = \{C_{ij}/i,j \in I_H\}$ denoting a patch of controlled cells (Fig. 1(b)), and $\bar{P} = \{C_{ij}/i,j \in I - I_H\}$ is the relative complement of P in Ω. In this section, control variables are introduced in the above mentioned model to control contacts between susceptibles of cells $C_{pq} \in P$ and infectives of cells $C_{rs} \in \bar{P} \cap V_{pq}$. For this, the model associated to a cell $C_{pq} \in P$, is given as follows

$$S_{i+1}^{C_{pq}} = S_i^{C_{pq}} - \beta_{pq} I_i^{C_{pq}} S_i^{C_{pq}} - \sum_{C_{rs} \in P \cap V_{pq}} \beta_{rs} I_i^{C_{rs}} S_i^{C_{pq}} - \sum_{C_{rs} \in \bar{P} \cap V_{pq}} u_i^{pqC_{rs}} \beta_{rs} I_i^{C_{rs}} S_i^{C_{pq}} - d S_i^{C_{pq}} \tag{11}$$

$$I_{i+1}^{C_{pq}} = I_i^{C_{pq}} + \beta_{pq} I_i^{C_{pq}} S_i^{C_{pq}} + \sum_{C_{rs} \in P \cap V_{pq}} \beta_{rs} I_i^{C_{rs}} S_i^{C_{pq}} + \sum_{C_{rs} \in \bar{P} \cap V_{pq}} u_i^{pqC_{rs}} \beta_{rs} I_i^{C_{rs}} S_i^{C_{pq}} - (d + \alpha + \gamma) I_i^{C_{pq}} \tag{12}$$

4.1. A vicinity travel restrictions optimal control approach on patches

We choose to minimize the following objective functional

$$J_P(u) = \sum_{C_{pq} \in P} A_{pq} I_N^{C_{pq}} + \sum_{i=0}^{N-1} \left(A I_i^{C_{pq}} + \sum_{C_{rs} \in \bar{P} \cap V_{pq}} \frac{A_{rs}}{2} (u_i^{pqC_{rs}})^2 \right)$$

where $u = \left(u_i^{pqC_{rs}}\right)_{C_{rs} \in \bar{P} \cap V_{pq}, i=0,...,N-1, p,q \in I_H}$. The goal is to minimize the infectives while minimizing the cost of vicinity travel restrictions control strategy in each cell C_{pq} in P. The minimization problem is taken over controls set,

$$U = \left\{ u \text{ measurable} / u^{min} \leq u_i^{pqC_{rs}} \leq u^{max},\ i = 1,...,N-1,\ C_{rs} \in \bar{P} \cap V_{pq} \right\}$$

where $u^{min} > 0$ and $u^{max} < 1$.

Then, we seek an optimal control $u^* = \left(u_i^{pqC_{rs}}\right)_{C_{rs} \in \bar{P} \cap V_{pq}, i=1,...,N-1, p,q \in I_H} \in U$ which minimizes the objective functional in above.

As done previously in the case of control of cells, we assume the existence of optimal controls and we derive the

necessary conditions based on the following Hamiltonian function

$$\begin{aligned} H = & \sum_{C_{pq}\in P}\Bigg[A_{pq}I_i^{C_{pq}} + \sum_{C_{rs}\in \bar{P}\cap V_{pq}} \frac{A_{rs}}{2}(u_i^{pqC_{rs}})^2 \\ & + \zeta_{1,i+1}^{C_{pq}}\Bigg[S_i^{C_{pq}} - \beta_{pq}I_i^{C_{pq}}S_i^{C_{pq}} - \sum_{C_{rs}\in P\cap V_{pq}}\beta_{rs}I_i^{C_{rs}}S_i^{C_{pq}} - \sum_{C_{rs}\in \bar{P}\cap V_{pq}} u_i^{pqC_{rs}}\beta_{rs}I_i^{C_{rs}}S_i^{C_{pq}} - dS_i^{C_{pq}}\Bigg] \\ & + \zeta_{2,i+1}^{C_{pq}}\Bigg[I_i^{C_{pq}} + \beta_{pq}I_i^{C_{pq}}S_i^{C_{pq}} + \sum_{C_{rs}\in P\cap V_{pq}}\beta_{rs}I_i^{C_{rs}}S_i^{C_{pq}} + \sum_{C_{rs}\in \bar{P}\cap V_{pq}} u_i^{pqC_{rs}}\beta_{rs}I_i^{C_{rs}}S_i^{C_{pq}} - (d+\alpha+\gamma)I_i^{C_{pq}}\Bigg]\Bigg] \end{aligned}$$

In the following, as done before, we announce the theorem of characterization of the optimal control u^* along with the necessary conditions

Theorem 4.1.
(Necessary Conditions)
Given an optimal control u^* and solutions $S^{C_{pq}*}$ and $I^{C_{pq}*}$, there exists $\zeta_{k,i}^{C_{pq}}$, $i = 0...N$, $k = 1,2$, the adjoint variables, for each cell C_{pq} in P, satisfying the following equations

$$\triangle\zeta_{1,i}^{C_{pq}} = -\Bigg[(1-d)\zeta_{1,i+1}^{C_{pq}} + \Bigg(\beta_{pq}I_i^{C_{pq}} + \sum_{C_{rs}\in P\cap V_{pq}}\beta_{rs}I_i^{C_{rs}} + \sum_{C_{rs}\in \bar{P}\cap V_{pq}} u_i^{pqC_{rs}}\beta_{rs}I_i^{C_{rs}}\Bigg)\Big(\zeta_{2,i+1}^{C_{pq}} - \zeta_{1,i+1}^{C_{pq}}\Big)\Bigg] \tag{13}$$

$$\triangle\zeta_{2,i}^{C_{pq}} = -\Big[A_{pq} + \beta_{pq}S_i^{C_{pq}}\Big(\zeta_{2,i+1}^{C_{pq}} - \zeta_{1,i+1}^{C_{pq}}\Big) + (1-d-\alpha-\gamma)\zeta_{2,i+1}^{C_{pq}}\Big] \tag{14}$$

where $\zeta_{1,N}^{C_{pq}} = 0, \zeta_{2,N}^{C_{pq}} = A$, are the transversality conditions. In addition

$$u_i^{pqC_{rs}*} = min\{max\{u^{min}, \frac{\Big(\zeta_{1,i+1}^{C_{pq}} - \zeta_{2,i+1}^{C_{pq}}\Big)\beta_{rs}I_i^{C_{rs}}S_i^{C_{pq}}}{A_{rs}}\}, u^{max}\},\ i = 0,...,N-1,\ C_{rs}\in\bar{P}\cap V_{pq} \tag{15}$$

Proof. Again, based on results in [23], and setting $S^{C_{pq}} = S^{C_{pq}*}$, $I^{C_{pq}} = I^{C_{pq}*}$ and $u^{pqC_{rs}} = u^{pqC_{rs}*}$ we obtain the following adjoint equations

$$\begin{aligned} \triangle\zeta_{1,i}^{C_{pq}} &= -\frac{\partial\mathscr{H}}{\partial S_i^{C_{pq}}} = -\Bigg[(1-d)\zeta_{1,i+1}^{C_{pq}} + \Bigg(\beta_{pq}I_i^{C_{pq}} + \sum_{C_{rs}\in P\cap V_{pq}}\beta_{rs}I_i^{C_{rs}} + \sum_{C_{rs}\in \bar{P}\cap V_{pq}} u_i^{pqC_{rs}}\beta_{rs}I_i^{C_{rs}}\Bigg)\Big(\zeta_{2,i+1}^{C_{pq}} - \zeta_{1,i+1}^{C_{pq}}\Big)\Bigg] \\ \triangle\zeta_{2,i}^{C_{pq}} &= -\frac{\partial\mathscr{H}}{\partial I_i^{C_{pq}}} = -\Big[A_{pq} + \beta_{pq}S_i^{C_{pq}}\Big(\zeta_{2,i+1}^{C_{pq}} - \zeta_{1,i+1}^{C_{pq}}\Big) + (1-d-\alpha-\gamma)\zeta_{2,i+1}^{C_{pq}}\Big] \end{aligned}$$

with $\zeta_{1,N}^{C_{pq}} = 0, \zeta_{2,N}^{C_{pq}} = A$. Then, we characterize the optimal control u^*, we need to differentiate the Hamiltonian with respect to the control at each cell C_{rs} at time i and set it equal to zero, i.e.

$$\frac{\partial H}{\partial u_i^{pqC_{rs}}} = A_{rs}u_i^{pqC_{rs}} - \zeta_{1,i+1}^{C_{pq}}\beta_{rs}I_i^{C_{rs}}S_i^{C_{pq}} + \zeta_{2,i+1}^{C_{pq}}\beta_{rs}I_i^{C_{rs}}S_i^{C_{pq}} = 0$$

Then, we obtain the optimal control

$$u_i^{pqC_{rs}} = \frac{\Big(\zeta_{1,i+1}^{C_{pq}} - \zeta_{2,i+1}^{C_{pq}}\Big)\beta_{rs}I_i^{C_{rs}}S_i^{C_{pq}}}{A_{rs}}$$

By the bounds in U of the control, it is easy to obtain $u_i^{pqC_{rs}*}$ in the following form

$$u_i^{pqC_{rs}*} = min\{max\{0, \frac{\Big(\zeta_{1,i+1}^{C_{pq}} - \zeta_{2,i+1}^{C_{pq}}\Big)\beta_{rs}I_i^{C_{rs}}S_i^{C_{pq}}}{A_{rs}}\}, u^{max}\},\ i = 0,...,N-1,\ C_{rs}\in\bar{P}\cap V_{pq}$$

□

4.2. Results II

In this section, we utilize the same data of Table 1. We note that we are interested here, to control the patch $P = \{C_{81}, C_{82}, C_{91}, C_{92}\}$. As supposed above in the case of control of cells, susceptibles are homogeneously distributed with 40 in each cell but except at the upper-right corner cell C_{19} now, and where we introduce 5 infectives and 35 susceptibles when the infection starts from the upper-right corner of Ω, and when it starts at the middle cell C_{55}.

Fig. 6(a) depicts behavior of susceptible individuals in Ω, and shows a remarkable decrease of susceptibles in P at $i = 600$ when the infection starts from C_{19}, while there is also a decrease of this number when the infection starts from C_{55} as seen in Fig. 6(b), which means that if the duration of the disease is longer, there would be a marked decrease of the number of susceptible individuals in the targeted patch.

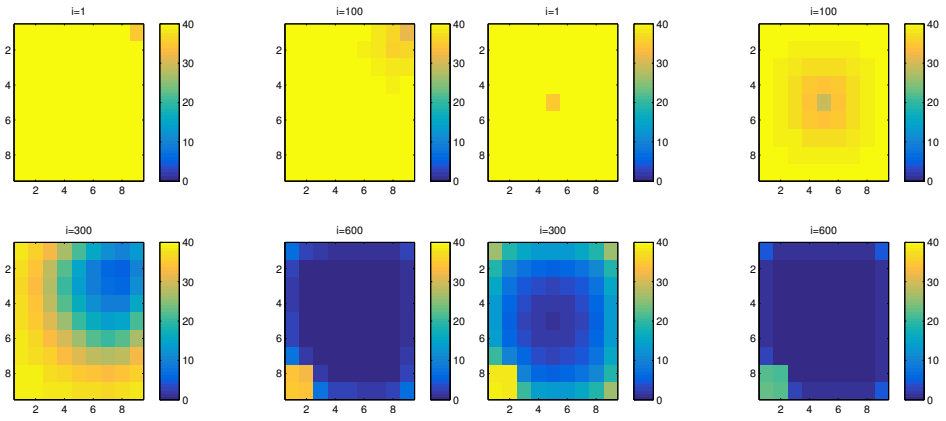

Fig. 6. Susceptibles behavior within Ω with controls. (a) When the infection starts from the upper-right corner cell C_{19}. (b) When the infection starts from the middle cell C_{55}.

Fig. 7(a) and Fig. 7(b) depict the behavior of the infected individuals in the absence of controls, and where we can compare the influence of the beginning of the infection on the number of infected individuals in the controlled patch. In fact, when the infection starts from the middle, there is an increase in the number of infected cases within P, compared to the case when the infection starts at the upper-right corner of Ω.

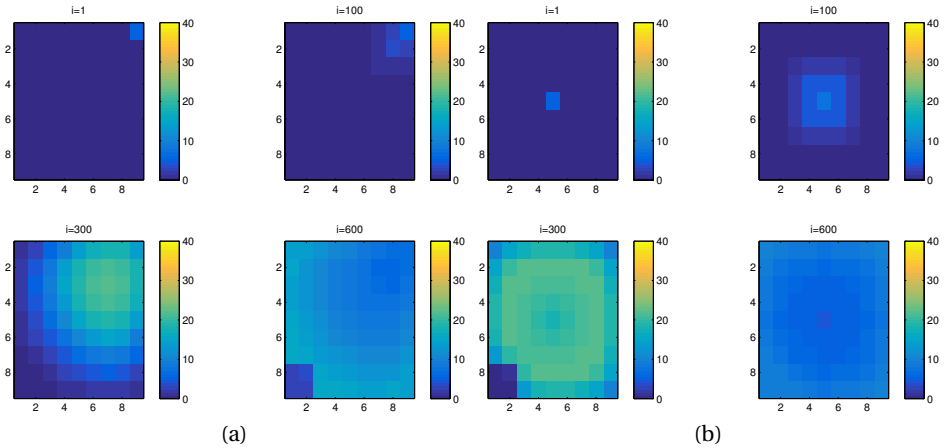

Fig. 7. Infectives behavior within Ω with controls. (a) When the infection starts from the upper-right corner cell C_{19}. (b) When the infection starts from the middle cell C_{55}.

It is observed from Fig. 8, that the controls severity weight A_{rs}, has an impact on the number of susceptible individuals, which means that, by an appropriate choice of A_{rs} ($A_{rs} = 50$), the number of susceptible individuals in P, remains more important, compared with the previous simulations, and regardless of the infection source.

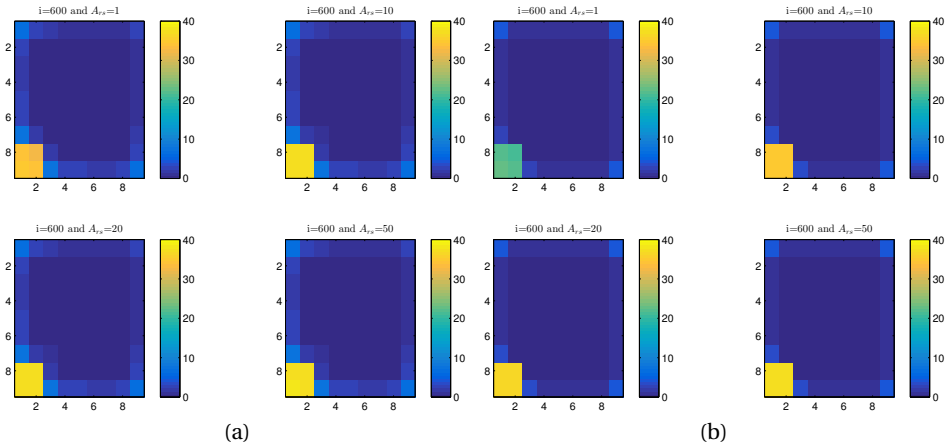

Fig. 8. Impact of A_{rs} on susceptibles of the controlled patch P at time $i = 600$ in the presence of controls. (a) When the infection starts from the upper-right corner cell C_{19}. (b) When the infection starts from the middle cell C_{55}.

In Fig. 9(a) and Fig. 9(b), we can observe that the number of infected individuals of P can be reduced effectively by changing the values of A_{rs}.

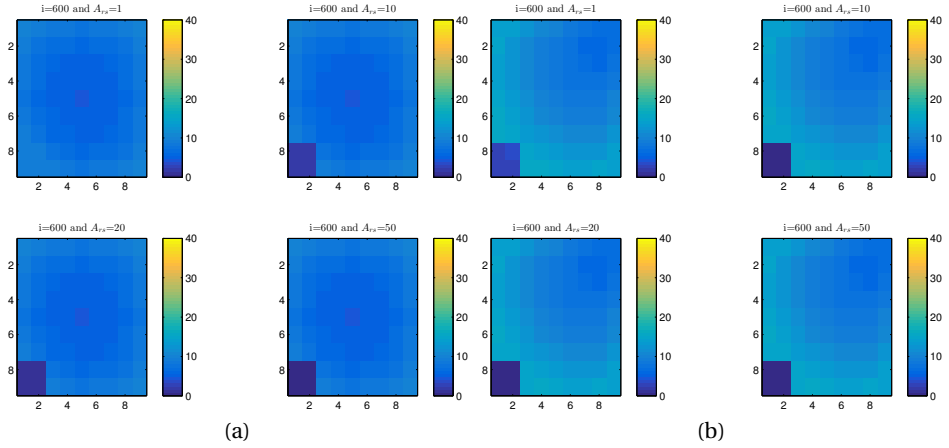

Fig. 9. Impact of A_{rs} on infectives of the controlled patch P at time $i = 600$ in the presence of controls. (a) When the infection starts from the upper-right corner cell C_{19}. (b) When the infection starts from the middle cell C_{55}.

We deduce from Fig. 8 and Fig. 9 that as more A_{rs} is bigger and far from 0, as more we can obtain satisfactory results regarding the evolution of the number of the susceptible people, and we obtain smaller numbers of infected people in P.

4.3. Results III: Patches in the interior of Ω

In the previous subsection, the controlled patches have been considered to be located at the lower-left corner of the grid. Here, we give an example of an other situation where the targeted patch P is located in the interior of Ω to investigate the effectiveness of the vicinity travel restrictions optimal control strategy when it is applied to a patch with a more important number of neighboring cells, for that, let consider a patch P defined by the set $P = \{C_{63}, C_{64}, C_{73}, C_{74}\}$.

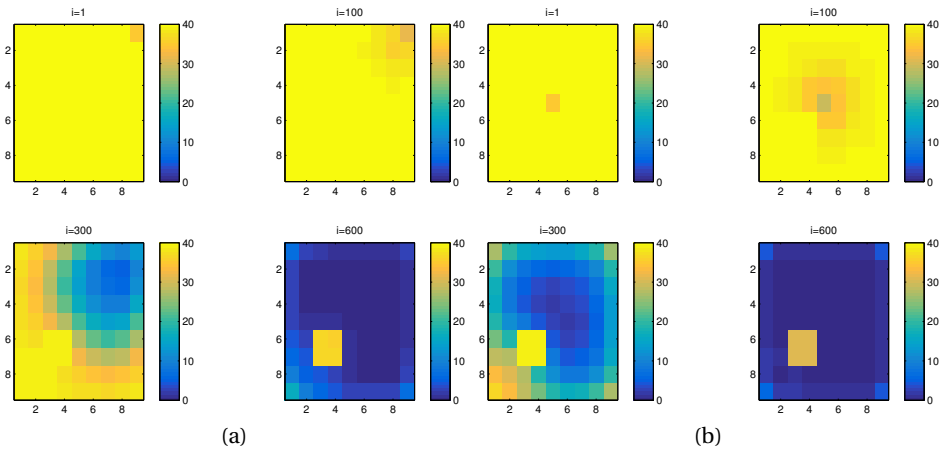

Fig. 10. Susceptibles behavior in the controlled patch P in the middle with the presence of controls and with $A_{rs} = 10$. (a) When the infection starts from the upper-right corner cell C_{19}. (b) When the infection starts from the middle cell C_{55}.

We can observe from Fig. 10 and Fig. 11, that the number of susceptible people in this situation, is less important than the one where the controlled patch has been considered at the corner (see Fig. 8, $A_{rs} = 10$), which means that, when the targeted patch are located in the interior of the studied domain Ω, more controls are needed.

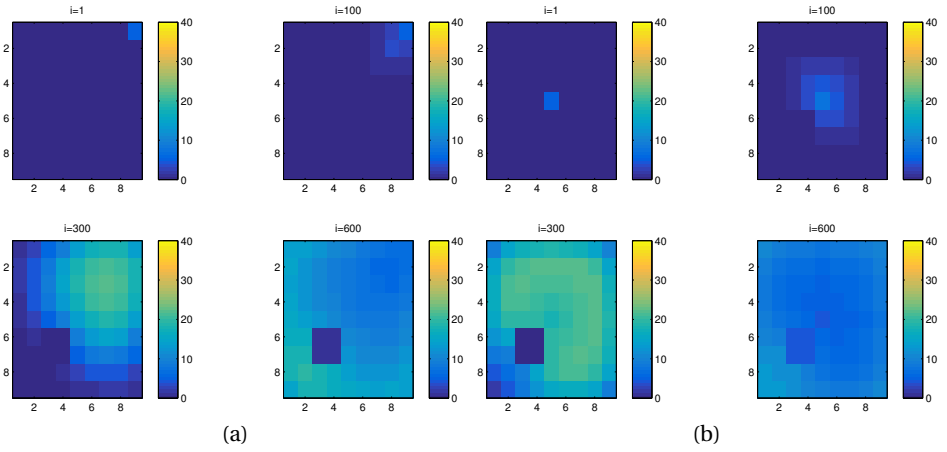

Fig. 11. Infectives behavior in the controlled patch P in the middle in the presence of controls and with $A_{rs} = 10$. (a) When the infection starts from the upper-right corner cell C_{19}. (b) When the infection starts from the middle cell C_{55}.

5. Conclusion

In this paper, we suggested two different optimal control problems for a discrete-time multi-regions SI epidemic model. In the first part of the study, only one cell C_{pq} with 8 neighbors, has been supposed to be the target of the vicinity travel restrictions optimal control strategy which aims to minimize the number of entered infectives and the cost of controls. As regards to the second part, we targeted a group of cells or entire patch P, once with 5 neighboring cells in the intersection between the vicinity of its cells and its complementary set, and an other time, with 8 neighbors, by following same logic of inter-interventions of the proposed control approach. Finally, we deduced that the suggested optimal control programs that are based on restriction of movements of infected people in vicinities of threatened regions, can effectively minimize the infection scale, either in cells or in patches.

References

[1] Kermack, W. O., McKendrick, A. G. (1927). A Contribution to the Mathematical Theory of Epidemics. Proceedings of the Royal Society A. 115 (772): 700-721. doi:10.1098/rspa.1927.0118.
[2] Zakary, O., Rachik, M., & Elmouki, I. (2016). On the impact of awareness programs in HIV/AIDS prevention: an SIR model with optimal control. Int. J. Comput. Appl, 133(9), 1-6.
[3] Zakary, O., Rachik, M., & Elmouki, I. (2017). How much time is sufficient for benefiting of awareness programs in epidemics prevention? A free final time optimal control approach. Int. J. Adv. Appl. Math. and Mech, 4(4), 26-40.
[4] Li, J., Teng, Z., Wang, G., Zhang, L., & Hu, C. (2017). Stability and bifurcation analysis of an SIR epidemic model with logistic growth and saturated treatment. Chaos, Solitons & Fractals, 99, 63-71.
[5] Zaman, G., Kang, Y. H., Cho, G., & Jung, I. H. (2017). Optimal strategy of vaccination & treatment in an SIR epidemic model. Mathematics and Computers in Simulation, 136, 63-77.
[6] Mpeshe, S. C., Nyerere, N., & Sanga, S. (2017). Modeling approach to investigate the dynamics of Zika virus fever: A neglected disease in Africa. Int. J. Adv. Appl. Math. and Mech, 4(3), 14-21.
[7] Kandhway, K., & Kuri, J. (2014). How to run a campaign: Optimal control of SIS and SIR information epidemics. Applied Mathematics and Computation, 231, 79-92.
[8] Safan, M., & Rihan, F. A. (2014). Mathematical analysis of an SIS model with imperfect vaccination and backward bifurcation. Mathematics and Computers in Simulation, 96, 195-206.
[9] Wu, Q., Lou, Y., & Zhu, W. (2016). Epidemic outbreak for an SIS model in multiplex networks with immunization. Mathematical biosciences, 277, 38-46.
[10] Liu, B., Duan, Y., & Luan, S. (2012). Dynamics of an SI epidemic model with external effects in a polluted environment. Nonlinear Analysis: Real World Applications, 13(1), 27-38.
[11] Tang, S. (2011). A modified SI epidemic model for combating virus spread in wireless sensor networks. International Journal of Wireless Information Networks, 18(4), 319-326.
[12] Romero-L, M., & Gallego, L. (2017). Analysis of voltage sags propagation in distribution grids using a SI epidemic model. In Power Electronics and Power Quality Applications (PEPQA), 2017 IEEE Workshop on (pp. 1-6). IEEE.
[13] Zakary, O., Rachik, M., & Elmouki, I. (2017). On the analysis of a multi-regions discrete SIR epidemic model: an optimal control approach. International Journal of Dynamics and Control, 5(3), 917-930.
[14] Zakary, O., Rachik, M., & Elmouki, I. (2017). A new analysis of infection dynamics: multi-regions discrete epidemic model with an extended optimal control approach. International Journal of Dynamics and Control, 5(4), 1010-1019.
[15] Zakary, O., Larrache, A., Rachik, M., & Elmouki, I. (2016). Effect of awareness programs and travel-blocking operations in the control of HIV/AIDS outbreaks: a multi-domains SIR model. Advances in Difference Equations, 2016(1), 169.
[16] Zakary, O., Rachik, M., & Elmouki, I. (2017). A multi-regional epidemic model for controlling the spread of Ebola: awareness, treatment, and travel-blocking optimal control approaches. Mathematical Methods in the Applied Sciences, 40(4), 1265-1279.
[17] Zakary, O., Rachik, M., & Elmouki, I. (2017). A new epidemic modeling approach: Multi-regions discrete-time model with travel-blocking vicinity optimal control strategy. Infectious Disease Modelling, 2(3), 304-322.
[18] Abouelkheir, I., Rachik, M., Zakary, O., & Elmouki, I. (2017). A multi-regions SIS discrete influenza pandemic model with a travel-blocking vicinity optimal control approach on cells. American Journal of Computational and Applied Mathematics, 7(2), 37-45.
[19] Abouelkheir, I., El Kihal, F., Rachik, M., Zakary, O., & Elmouki, I. (2017). A multi-regions SIRS discrete epidemic model with a travel-blocking vicinity optimal control approach on cells. Br. J. Math. Comput. Sci, 20(4), 1-16.
[20] El Kihal, F., Rachik, M., Zakary, O., & Elmouki, I. (2017). A multi-regions SEIRS discrete epidemic model with a travel-blocking vicinity optimal control approach on cells. Int. J. Adv. Appl. Math. Mech, 4(3), 60-71.
[21] El Kihal, F., Abouelkheir, I., Rachik, M., & Elmouki, I. Optimal Control and Computational Method for the Resolution of Isoperimetric Problem in a Discrete-Time SIRS System. Mathematical and Computational Applications, 23(4), 52. (2018).
[22] Zakary, O., Rachik, M., Elmouki, I., & Lazaiz, S. (2017). A multi-regions discrete-time epidemic model with a travel-blocking vicinity optimal control approach on patches. Advances in Difference Equations, 2017(1), 120.
[23] Sethi, S. P., & Thompson, G. L. (2000). What is optimal control theory? (pp. 1-22). Springer US.